Localization of HDAC1 using high resolution microscopy

Karin Abarca Heidemann[*1], Sarah Crowe[*2], Tobias Jacob[2], Carl A. Ascoli[1]
*Contributed equally. [1]Rockland Immunochemicals Inc., Limerick, PA, [2]Leica Microsystems, West Chester PA
Correspondence to K. Abarca Heidemann: karin.abarca@rockland-inc.com, 1-800-656-7625

ABSTRACT

The fundamental patterns of epigenetic components, such as DNA methylation and histone modifications, are frequently altered in tumor cells. Acetylation is one of the best characterized modifications of histones, which is controlled by histone acetyltransferases (HATs) and histone deacetylases (HDACs). HDAC enzymes are involved in removing the acetyl group from histones in nucleosomes. HDACs are involved in modulating most key cellular processes, including transcriptional regulation, apoptosis, DNA damage repair, cell cycle control, autophagy, metabolism, senescence and chaperone function. In general, hyperacetylation is associated with increased transcriptional activity, whereas decreased levels of acetylation (hypoacetylation) is associated with repression of gene expression. Steady-state levels of acetylation of core histones result from the balance between the opposing activities of histone acetyltransferases and histone deacetylases (HDACs). In addition to deacetylation of histones, HDACS also are known to deacetylate other proteins including p53, tubulin, E2F, GATA1, STAT3, NF-kB, SMAD7, MyoD among others.
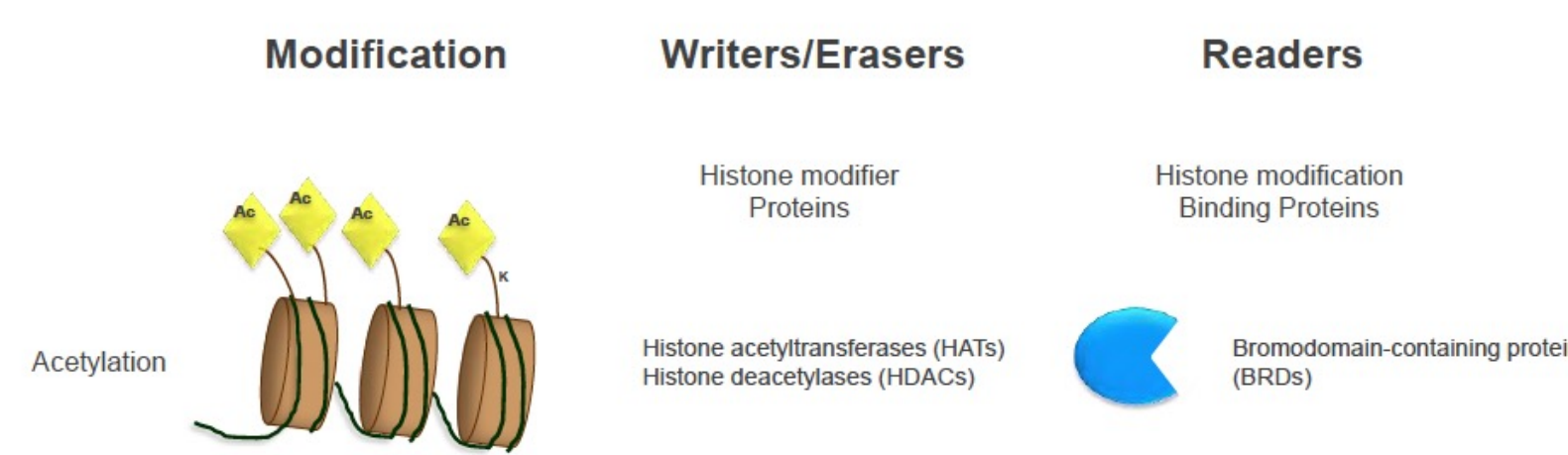
Figure 1: Schematic drawing depicting the players in the histone acetylation/deacetylation process.

INTRODUCTION

Eighteen distinct HDACs have been identified to date. They are classified into four groups based on their structural divergence, namely class I, II, III and IV HDACs (see Table 1). The first two classes are considered "classical" HDACs whose activities are inhibited by trichostatin A (TSA), whereas the third class is a family of NAD+- dependent proteins not affected by TSA.

Homologues to these three classes are found in yeast having the names: reduced potassium dependency 3 (Rpd3), which corresponds to Class I; histone deacetylase 1 (hda1), corresponding to Class II; and silent information regulator 2 (Sir2), corresponding to Class III. Class IV (HDAC11) is homologous with class I and class II enzymes. The Class III group is considered an atypical category of its own, which are NAD+-dependent, whereas other groups require Zn2+ as a cofactor. The function and activity of HDACs vary depending on their structure and intracellular localization. The importance of HDACs in the regulation of cellular activities under physiological and diseased conditions makes HDACs critical targets in in the treatment of cancer and inflammatory disorders. Understanding their cellular function, localization and their inhibition is crucial for cancer research and therapeutics.

Immunohistochemistry (IHC) analysis of tissue samples (Figures 2-4) is essential for the detection of the protein in a sample and is often used in diagnostic experiments, but does not result in an image that will allow co-localization experiments.

Classification	HDAC	Subcellular localization
I	HDAC1	Nucleus
	HDAC2	Nucleus
	HDAC3	Nucleus
	HDAC8	Nucleus
IIa	HDAC4	Nucleus/cytoplasm
	HDAC5	Nucleus/cytoplasm
	HDAC7	Nucleus/cytoplasm
	HDAC9	Nucleus/cytoplasm
IIb	HDAC6	Mostly cytoplasm
	HDAC10	Nucleus/cytoplasm
III	SIRT1	Nucleus/cytoplasm
	SIRT2	Cytoplasm
	SIRT3	Nucleus/mitochondria
	SIRT4	Mitochondria
	SIRT5	Mitochondria
	SIRT6	Nucleus
	SIRT7	Nucleolus
IV	HDAC11	Nucleus/cytoplasm

Table 1: HDAC overview and localization.

Studying protein localization within a cell requires precise high-resolution imaging techniques. Confocal microscopy can provide information on subcellular localization, achieving up to 200nm resolution. Additionally, optical sectioning of multiple image planes on a confocal allows for the study of protein location in a volume. With the introduction of the Leica SP8. STED 3X (Stimulated Emission Depletion) super-resolution microscope, subcellular localization can now be performed in the sub-50 nm range, breaking the diffraction limit. The use of STED super-resolution microscopy can give new insight into the localization and function of individual HDAC family members and other corresponding molecules.

Figure 2: Immunohistochemistry of HDAC1 in human prostate cancer tissue. Cellular localization of HDAC1 is nuclear (purple precipitate).

Figure 3: Immunohistochemistry of HDAC5 in colon tissue. Cellular localization of HDAC5 in this tissue is nuclear with some cytosolic appearance (red precipitate).

Figure 4: Immunohistochemistry of HDAC10 in testis tissue. Cellular localization of HDAC10 in this tissue is cytoplasmic and nuclear (red precipitate).

The use of high specificity and high affinity antibodies is critical in any localization experiment to assure the positive outcome of the assay. Quality control is essential in the development and manufacture of such antibodies allowing visual evidence of proper target localization and low background staining. Here we present staining and compare high resolution localization of HDAC1 analysis performed on a confocal microscope to STED microscopy. HDAC1 has been shown to be involved in the suppression of a number of genes implicated in multi-lineage blood cell development and to be required for the transcriptional repression of circadian target genes, such as PER1, mediated by the large PER complex or CRY1 through histone deacetylation. HDAC1 together with MAT2 deacetylates p53 and modulates its effect on cell growth and apoptosis.
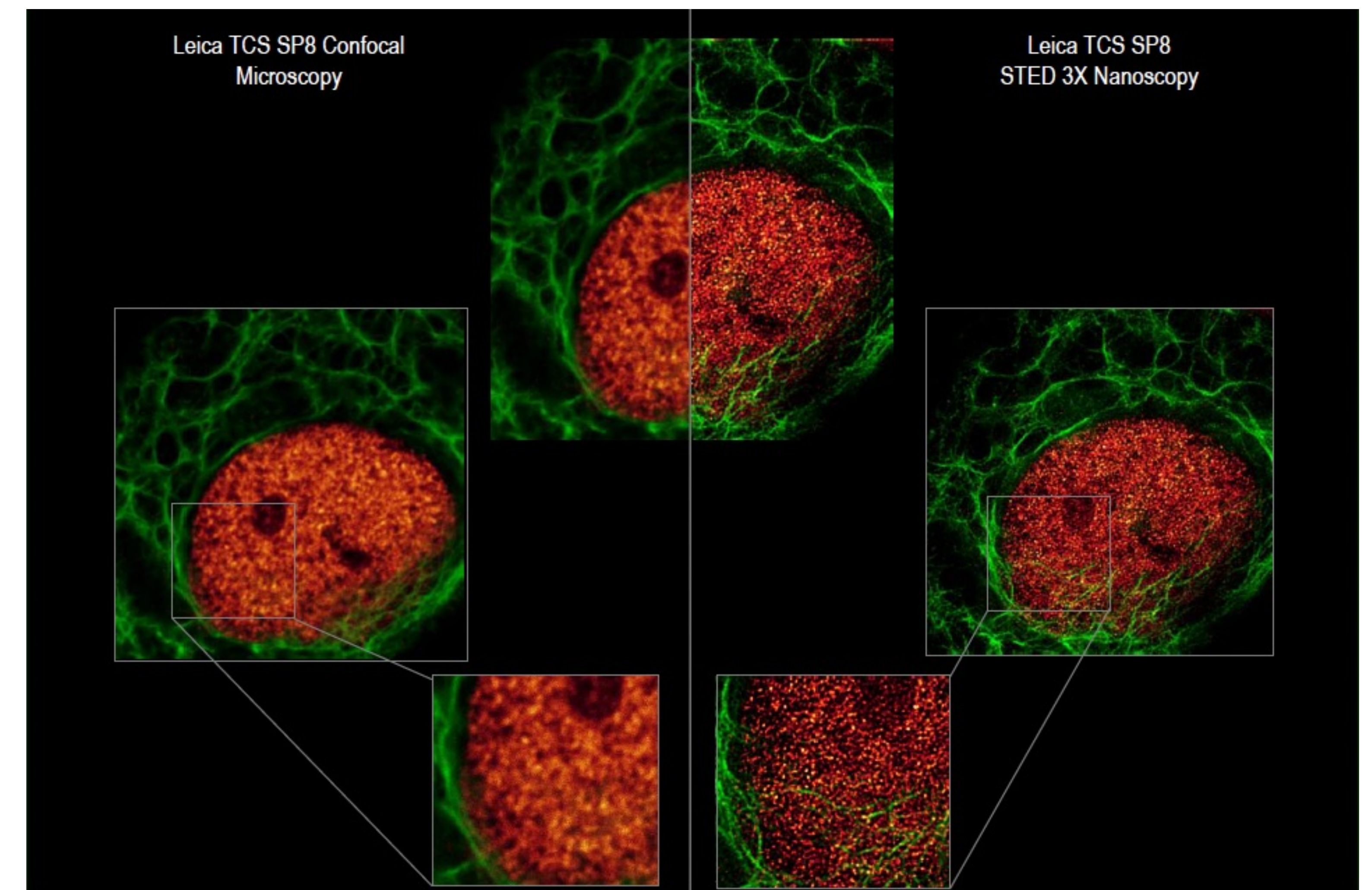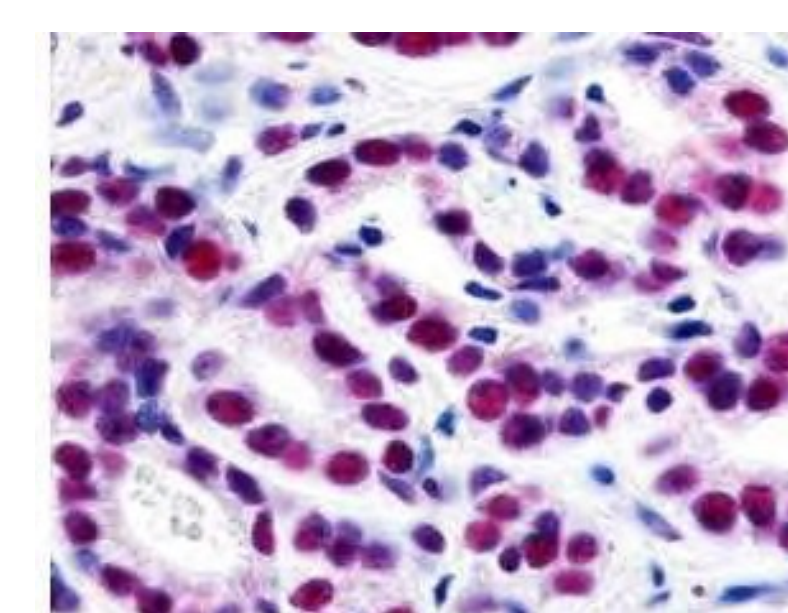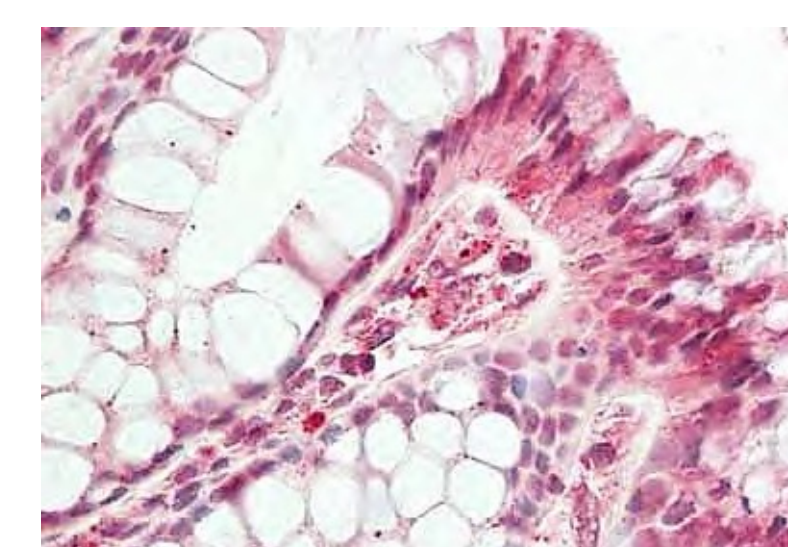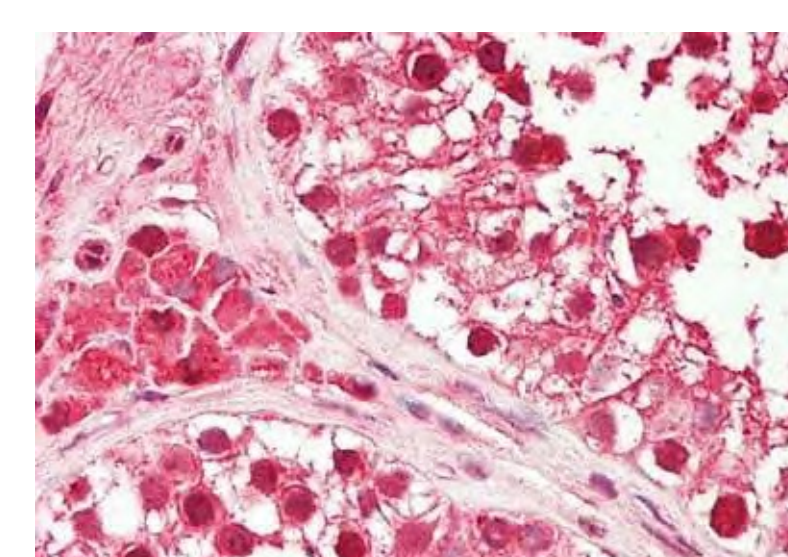
LOCALIZATION OF HDAC1 & KERATIN

Figure 5: Confocal vs STED imaging. Epidermoid carcinoma cell line A431 stained for HDAC1-ATTO 550 (red) and Keratin-DyLight 488 (green). The same cell was imaged using standard confocal imaging (left) and STED 3X imaging (right). HDAC1 localizes at the nucleolar periphery.

STED MICROSCOPY

Stimulated Emission Depletion (STED) microscopy is a confocal super-resolution imaging technique. STED super-resolution is obtained by overlaying an excitation laser and a depletion laser to achieve an optical "sculpting" of the point spread function (PSF), which is then raster scanned over the field of view. The depletion laser beam is introduced in to the light path to create a "donut" shape, which is aligned and overlaid with the excitation beam (Fig. 6).

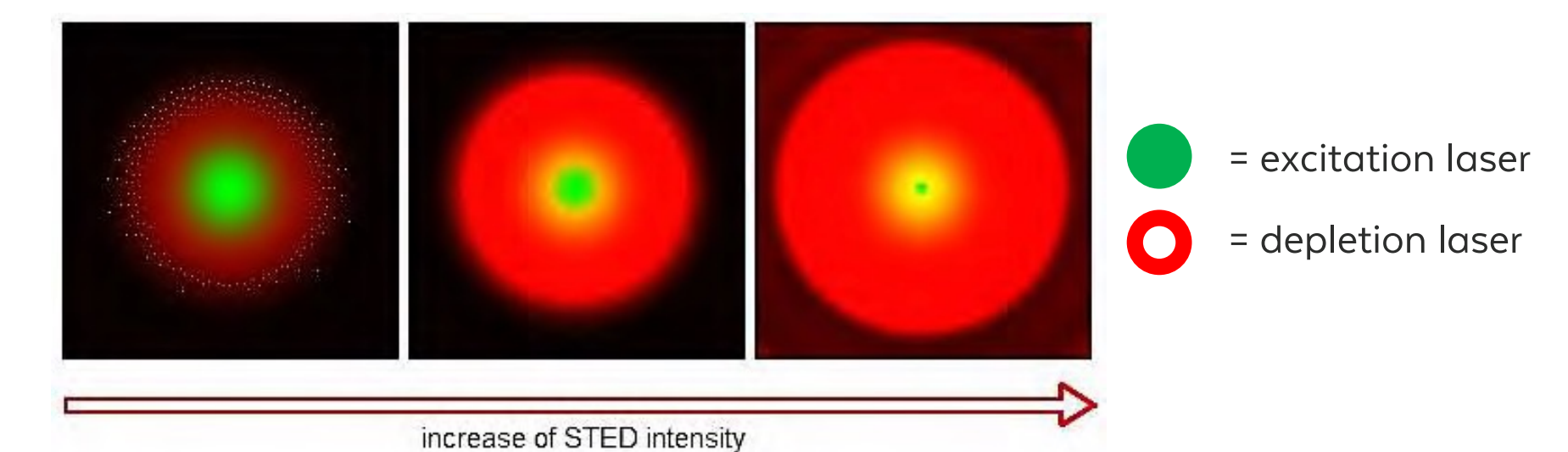

= excitation laser
= depletion laser

Figure 6: The excitation beam and STED depletion beam

The donut depletion laser de-excites the fluorophores through stimulated emission process while leaving the molecules in the donut hole to go through normal fluorescence process. By increasing the depletion laser power the size of the donut hole where normal fluorescence process occurs decreases. Utilization of time gating, which takes advantage of the fluorescence lifetime differences between normal fluorescence and stimulated emission, further enhances the resolution down to 40nm. Two of the major advantages of STED compared to other super-resolution techniques is a purely optical resolution improvement, without post-processing, and the ability to use optical sectioning. The Leica TCS SP8 STED 3X is available with a 592 nm depletion laser and/or a 660 nm depletion laser. The 592 nm depletion beam is best suited for dyes that are in the green spectral range (Fig. 7), such as DyLight 488, while the 660 nm depletion laser is recommended for dyes that emit in the yellow to orange range (Fig. 7), such as ATTO 550
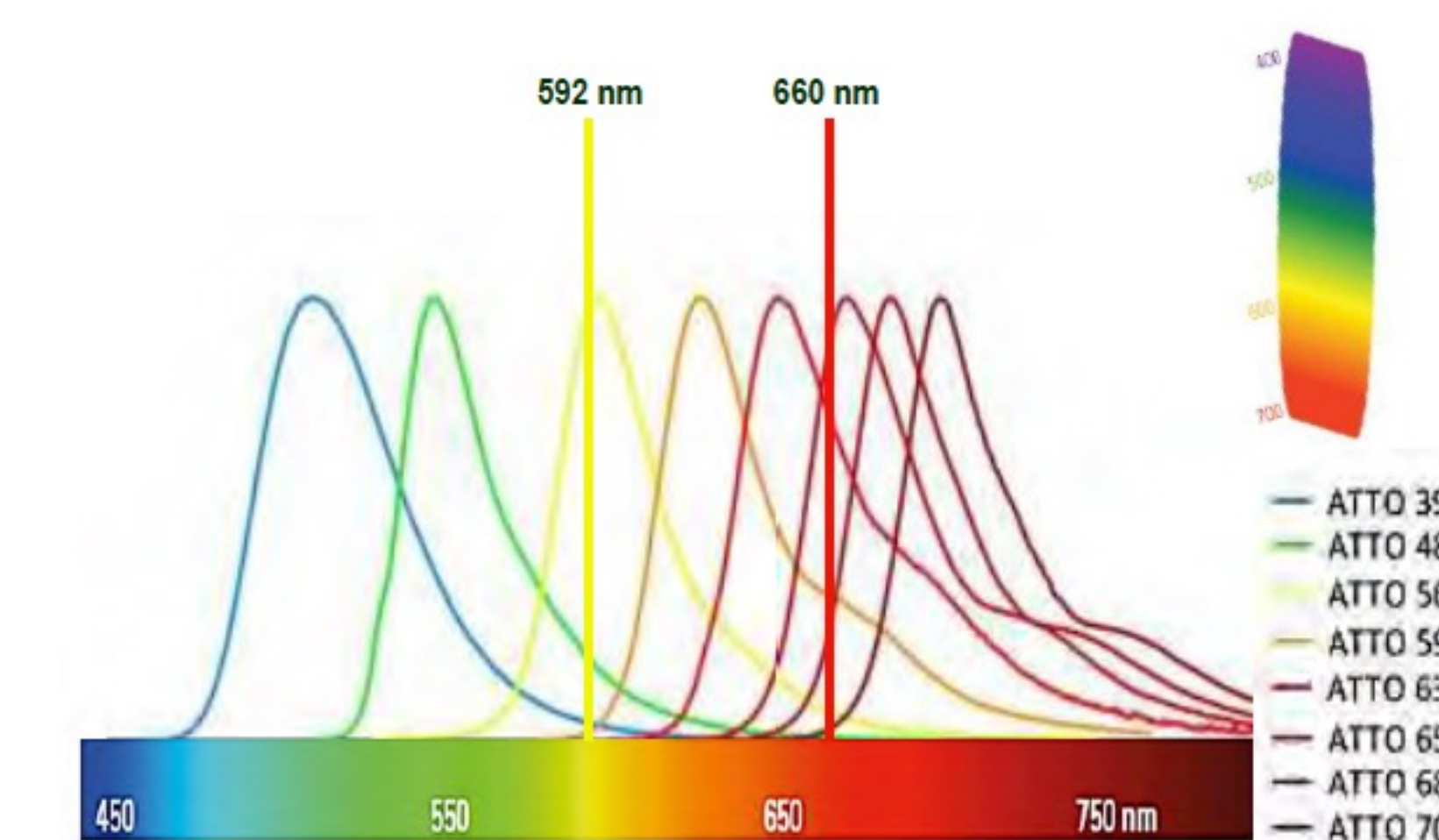

Figure 7: Dye spectra examples from ATTO with the Leica STED lasers at 592 nm and 660 nm

CONCLUSIONS & FUTURE DEVELOPMENT

Here we show staining of HDAC1 in cancer tissue (Figure 2) and epidermoid carcinoma cells (Figure 5). HDAC1 localization in the analyzed samples was confirmed to be nuclear. Cytosolic staining of HDAC1 reported to occur in certain cancer samples was not observed. Using STED microscopy compared to confocal imaging showed a visible increase in resolution (Figure 5). These results clearly show that the use of appropriate validated antibodies and STED microscopy are important tools to study subcellular structures beyond the diffraction limit correcting ill-defined images. This is critical in co-localization studies of proteins inside cells. It is still to be determined in future experiments if STED microscopy can resolve co-localization of HDAC proteins with acetylated groups on histones or other proteins.

REFERENCES

1. Li Z, Zhu WG. Targeting Histone Deacetylases for Cancer Therapy: From Molecular Mechanisms to Clinical Implications. Int J Biol Sci. 2014 Jul 2;10(7):757-770

2. De Ruijter A, Van Gennip A, Caron H, Kemp S, van Kuilenburg A. Histone deacetylases (HDACs): characterization of the classical HDAC family. Biochem J. 2003;370:737-749.

3. Blander G, Guarente L. The Sir2 family of protein deacetylases. Annu Rev Biochem. 2004;73:417-435.

4. Xu W, Parmigiani R, Marks P. Histone deacetylase inhibitors: molecular mechanisms of action. Oncogene. 2007;26:5541-5552.

5. Marks PA, Rifkind RA, Richon VM, Breslow R, Miller T, Kelly WK. Histone deacetylases and cancer: causes and therapies. Nat Rev Cancer. 2001;1:194–202

6. Minucci S, Pelicci PG. Histone deacetylase inhibitors and the promise of epigenetic (and more) treatments for cancer. Nat Rev Cancer. 2006;6:38–51

7. Robert T, Vanoli F, Chiolo I, Shubassi G, Bernstein KA, Rothstein R. et al. HDACs link the DNA damage response, processing of double-strand breaks and autophagy. Nature. 2011;471:74–9.

8. Kim JY1, Shen S, Dietz K, He Y, Howell O, Reynolds R, Casaccia P. HDAC1 nuclear export induced by pathological conditions is essential for the onset of axonal damage. Nat Neurosci. 2010 Feb;13(2):180–9.

9. Hell SW, Wichmann J. Breaking the diffraction resolution limit by stimulated emission: stimulated-emission-depletion fluorescnece microscopy. Opt Lett. 1994 Jun;19(11):780-2.

10. Donnert G, Keller J, Wurm CA, Rizzoli SO, Westphal V, Schonle A, Jahn R, Jakobs S, Eggeling C, Hell SW. Two-color far-field fluorescence nanscopy. Biophys J. 2007 Apr;92(8):L67-9.

METHODS

IHC: Sample tissue was fixated by formalin fixed paraffin embedding. Protein detection was performed using primary antibodies at 5 μg/mL (HDAC5 and HDAC10) or 1:500 (HDAC1) for 1 h at room temperature. Secondary antibody: peroxidase rabbit secondary antibody (Rockland, p/n 611-103-122) at 1:10,000 for 45 min at room temperature. Proteins were visualized as precipitated red or purple signal with hematoxylin purple or blue nuclear counterstain. Primary antibodies shown: HDAC1 (Rockland, p/n 600-401- 879), HDAC5 (Rockland, p/n 600-401-J69) and HDAC10 (Rockland, p/n 600-401-J75).

Conditions for STED microscopy: A431 cells (ATCC CRL-1555) were incubated at 37°C with 5% CO2 in Dulbecco's Modified Eagle Medium (DMEM, Invitrogen, MO) with 10% FBS (Rockland, p/n FBS-01-0500) in 25 cm2 cell culture flask. When cells reached 70 to 80% confluence, they were detached using TrypLE (Invitrogen, MO), and then placed on # 1.5 coverslips in 6 wells plates until reaching ~30% confluency. Cells were fixed using ice-cold (-20°C) methanol for 7 minutes. Once fixed, cells were rinsed in PBS at room temperature and then incubated in blocking solution for 15 minutes (PBS/Normal Goat Serum 10%, Triton-X100 at 0.2%). This step was followed by incubation with the following primary antibodies for 1 hour at room temperature: rabbit anti-HDAC1 1:50 (Rockland, p/n 600-401-879) and mouse anti-Keratin 1:50 (Rockland, p/n 200-301-390). Cells were rinsed three times in PBS for 10 minutes/rinse, and then incubated in blocking solution for 15 minutes. DyLight 488 anti-Mouse IgG (Rockland, p/n 610-141-002) and ATTO 550 anti-Rabbit IgG (Rockland, p/n 611-154-122) were diluted 1:100 each in blocking solution and incubated for one hour. Cells were rinsed in PBS three times and then in tap water once. Coverslips were then mounted in ProLong Antifade Kit (Life Technologies, p/n P-7481) and allowed to cure in the dark for at least 3 days. It is important to wait at least 3 days, as it takes time for ProLong products to reach the desired refractive index (RI of 1.46) for imaging. The slides were examined using a TCS SP8 STED 3X microscope (Leica Microsystems, Inc.) using a white light laser tuned to 470nm to excite the DyLight 488 fluorescence and 550nm to excite the ATTO 550. For STED images, DyLight 488 was used with the 592nm depletion laser set to 95% power with a time gating range of 1.5-6.0 ns, and ATTO 550 was used with the 660nm depletion laser set to 100% power with a time gating range of 1.5-6.0 ns..